Inorganica Chimica Acta 510 (2020) 119777

Contents lists available at ScienceDirect

Inorganica Chimica Acta

journal homepage: www.elsevier.com/locate/ica

Research paper

Synthesis and electrochemical investigation of chiral amine bis(phenolate)-boron complexes: *In vitro* antibacterial activity screening of boron compounds

Ahmet Kilic[a,b,*], Levent Beyazsakal[a], Bahar Tuba Findik[c], Hilal Incebay[d]

[a] Harran University, Faculty of Arts and Science, Department of Chemistry, Sanliurfa 63290, Turkey
[b] Research Centre for Science and Technology, Harran University, Sanliurfa 63290, Turkey
[c] Nevsehir Hacı Bektas Veli University, Faculty of Arts and Sciences, Department of Chemistry, Nevsehir 50300, Turkey
[d] Nevsehir Hacı Bektas Veli University, Faculty of Arts and Sciences, Department of Molecular Biology and Genetics, Nevsehir 50300, Turkey

ARTICLE INFO

Keywords:
Chiral amine bis(phenolate) ligand
Chiral boron complexes
Spectroscopy
Electrochemistry
Antibacterial activity

ABSTRACT

A new class of low-cost, easily-synthesizable and modifiable chiral amine bis(phenolate) ligand **(L),** its chiral boron complex **(LB),** and five different salen groups (1-(3-Aminopropyl) imidazole **(LB_1)**, *N,N*-Diethyl-*p*-phenylenediamine **(LB_2)**, 2-Picolylamine **(LB_3)**, 4′-Aminoacetophenone **(LB_4),** and 4-Amino-2,2,6,6-tetramethyl piperidine **(LB_5)**) containing chiral boron complexes were synthesized in this study. These newly synthesized chiral compounds were fully characterized by ^{1}H and ^{13}C NMR, FT-IR, UV–Vis, and LC-MS/MS spectroscopy, melting point, elemental analysis, and cyclic voltammetry techniques. The *in vitro* antibacterial activity of the synthesized different chiral boron complexes was tested against four pathogenic bacteria strains using the resazurin-based broth microdilution method, and the MIC values of each boron complex were determined. Based on the overall results, the *N, N*-Diethyl-*p*-phenylenediamine group containing chiral boron complex **(LB_2)** showed the highest activity against all bacterial strains, with the lowest MIC value of 4 μg/mL which is nearly in the range of values for commercial antibacterial drugs.

1. Introduction

Boron-based organic synthesis has become one of the most popular research areas due to the unique coordination chemistry of boron which allows the preparation of functionalized novel compounds. The design and spectroscopic properties of different boron derivatives have been extensively studied in organic synthesis, and different boron-based applications in various fields such as catalytic [1–3], fluorescence [4], electrochemical [5], pharmaceutical [6–8], enzyme-based detection [9], photo and electroluminescent devices [10] have been described by other research groups. As a relatively new focus area, boron derivatives have been used in designing new therapeutic agents based on biological activities of boron compounds which depend on the chemistry of boron atom [11,12]. Due to its vacant p-orbital, boron is a strong Lewis acid and could drive the formation of a dative bond (coordinate covalent bond) with a pair of electrons on the hydroxyl and amine groups of amino acid residues, carbohydrates and nucleic acids [13–16].

Boronic acids are a class of boron-containing compounds that are used for the preparation of complex molecules [17]. A boronic acid is a trivalent boron-containing compound that has two hydroxyls and one alkyl or aryl functional groups. The functional group bonded to boron determines the reactivity of boronic acid [18,19]. Their unique reactivity (mild organic Lewis acids), stability, and low toxicity make boronic acids widely applicable as synthetic intermediates in different areas [20,21]. These compounds have been used as building blocks for crystal engineering [22] and the generation of supramolecular architectures, possible enzyme inhibitors, and therapeutics [23] due to their unique electronic structure [24–26]. Several boronic acid derivatives have been used to design new drugs over the past decades. Boron-containing compounds have been explored as inhibitors for different biological targets and some of them were approved by Food and Drug Administration (FDA) as the drugs to treat a variety of diseases such as multiple myeloma, cancer, etc [27,28]. Moreover, many of them are good candidates for designing potential antimicrobial agents. An approved cyclic boronic acid derivative has been used to treat urinary tract infections. The mechanism of the drug relies on the inhibition of β-lactamase enzymes which is the source of bacterial resistance [29–31].

Usage of different polydentate ligands plays a significant role in the

* Corresponding author at: Harran University, Art and Science Faculty, Chemistry Department, TR-63290 Sanlıurfa, Turkey.
E-mail address: kilica63@harran.edu.tr (A. Kilic).

https://doi.org/10.1016/j.ica.2020.119777
Received 26 March 2020; Received in revised form 12 May 2020; Accepted 17 May 2020
Available online 19 May 2020
0020-1693/

improvement of the structure and reactivity of the metal complexes. Tetradentate ligands have become an important part of today's chemistry in order to generate functionalized novel compounds [32,33]. The use of chelating tetradentate amine-bis(phenolate) ligands has recently played an increasingly important role in transition-metal catalyst design and modeling of metalloenzyme active-sites. During several years we have studied the different behavior exhibited by these ligands, mainly due to the potential reduction capacity showed by the chemical group which leads to a great variety of coordination patterns [34]. Chiral amine-bis(phenolate) ligand which is a chelating tetradentate has been an attractive subject in combination with various metals such as Fe, Co, Rh, Zr, and Cr and these metal complexes have been acted as catalysts for cross-coupling of alkyl halides [35–39], 1-hexene polymerization [40], hydrogenation of ketones [37] and CO_2 conversion [41]. To the best of our knowledge, the synthesis and applications in different fields of chiral amine bis(phenolate)-boron complexes are very rare. The reason for choosing tetradentate amine-bis(phenolate) ligands containing valinol and salen group in this study, these ligands have enhanced flexibility, solution processability at low cost and further structural manipulation properties. Also, the azomethine group (C═N) has been proven to play a critical role in biological activities of salen compounds and their antimicrobials activities have been enhanced when complexing with boron [42]. In addition, (B ← N) and (B-O) units containing boron-nitrogen compounds have antimicrobial activities [43].

To the best of our knowledge, the synthesis and applications in different fields of chiral amine bis(phenolate)-boron complexes are very rare. To fill the gap, herein we reported the synthesis, characterization and *in vitro* antibacterial activities of chiral amine bis(phenolate) ligand **(L),** its chiral boron complex **(LB)** and five different salen groups (1-(3-Aminopropyl) imidazole **(LB_1)**, *N,N*-Diethyl-*p*-phenylenediamine **(LB_2)**, 2-Picolylamine **(LB_3)**, 4′-Aminoacetophenone **(LB_4),** and 4-Amino-2,2,6,6-tetramethyl piperidine **(LB_5)**) containing chiral boron complexes. The structures of all newly synthesized complexes were assigned by the ^1H and ^{13}C NMR, FT-IR, UV–Vis spectroscopy, LC-MS/MS spectrometry, and cyclic voltammetry technique as well as elemental analysis. The *in vitro* antibacterial activity of compounds was determined against *Escherichia coli* (ATCC 25922), *Bacillus cereus* (ATCC 11778), *Staphylococcus aureus* (ATCC 25923), and *Listeria monocytogenes* (ATCC 7644) using the broth microdilution method.

2. Experimental section

2.1. General considerations

All organic solvents and starting materials used in the study were obtained from commercial suppliers and used as received. Since a dry atmosphere is required, synthesis of chiral boron complex **(LB)** was performed under the Ar atmosphere and a Dean-Stark apparatus was used to remove the water formed during the reaction. The formation of chiral amine bis(phenolate) ligand **(L)**, its chiral boron complexes **(LB),** and salen group containing chiral boron complexes **($LB_{(1-5)}$)** were studied using an FT-IR spectrophotometer (Perkin-Elmer Two UATR-FT-IR) and the results were recorded in the range of 4000 to 400 cm^{-1} at 25 °C equipped with ATR accessory. The electronic absorption spectra of the synthesized compounds were measured in C_2H_5OH-$CHCl_3$ solvent within the range of 200 to 1100 nm using a UV–Vis spectrophotometer (Perkin-Elmer model Lambda 25, with 1 cm quartz cuvettes) at 25 °C. The ^1H NMR (400 MHz) and ^{13}C NMR (100 MHz) spectra in $CDCl_3$ solution were recorded on an Agilent Technologies and spectral results were recorded using TMS as an internal reference. Chemical shifts were reported in delta (δ) units, parts per million (ppm) downfield from TMS, and *J* values were given in Hertz. Mass spectra (MS) were measured using an LC-MS/MS system consisting of a Quadrupole-Orbitrap Mass Spectrometer (Shimadzu LCMS-8030 series) under electrospray ionization (ESI) technique. Elemental analyses for C, H, and N were performed on a thermos scientific CHNS/O FlashSmart model elemental analyzer. Thin-layer chromatography (TLC) was conducted on glass plates coated with silica gel. Melting points of all chiral amine bis(phenolate)-boron complexes have been determined in open capillary tubes on an Electrothermal 9100 melting point apparatus and were not corrected. For the electrochemical studies of the chiral boron complex **(LB),** and salen group containing chiral boron complexes **($LB_{(1-5)}$)**, the anodic and cathodic potential was measured in deoxygenated (N_2) acetonitrile solution containing 0.10 M tetrabutylammonium tetrafluoroborate (TBATFB) in the presence of 0.01 M ferrocene as supporting electrolyte on a Gamry Interface 1000B Potentiostat/Galvanostat/ZRA equipped with a three-electrode electrochemical cell with a glassy carbon working electrode (0.00785 cm^2), a Pt wire counter electrode and an Ag/Ag^+ reference electrode. The Ag/Ag^+ electrode used as non-aqueous media reference electrode was prepared with 0.01 M $AgNO_3$ and 0.10 M TBATFB in CH_3CN. The potential range was determined as −0.2/1.5 V and CV experiments were performed using 1 mM concentrations of each complex at a scan rate of 50 mVs^{-1}.

2.2. Synthesis of chiral amine bis(phenolate) ligand (L)

A solution of 4-*tert*-butyl phenol (2.40 g, 16.0 mmol), (R)-(-)-2-Amino-3-methyl-1-butanol (0.83 g, 8.0 mmol), and 36% aqueous formaldehyde (1.5 mL, 20.16 mmol) in ethanol/water (35 + 15 mL, respectively) was slowly added to a 100 mL two-necked round-bottom flask at 25 °C and the solutions or mixture were refluxed for 24 h. After cooling the homogeneous solution to room temperature, a yellow oily chiral amine bis(phenolate) ligand **(L)** occurred. $CHCl_3/C_2H_5OH$ (1:3) was used as a solvent for the crystallization of the ligand **(L)**. To obtain crystals of oily chiral ligand **(L)**, the solvent was evaporated slowly. However, solid crystal products could not be obtained. Therefore, some spectroscopic properties of the ligand could not be examined.

Chiral ligand (L): Elemental Analysis (calculated for $C_{27}H_{41}NO_3$) (F.W: 427.6 g/mol) (%): C, 75.84; H, 9.66; N, 3.28. Found: C, 75.80; H, 9.61; N, 3.33. FT-IR (ATR, υ_{max}-cm^{-1}): 3580–3142 υ(Ar-OH···N), 3064 and 3029 υ(Ar-CH), 2960–2872 υ(Aliph-CH), 1614–1597 υ(*o*-phenolate-C═C), 1520–1462 υ(C═C), 1128 υ(C−O). ^1H NMR (400 MHz; $CDCl_3$): *δ* (ppm) = 8.41 (s, 2H, Ar-OH), 7.30 (d, 2H, *J* = 8.0 Hz, Ar-C*H*), 7.08 (s, 2H, Ar-C*H*), 6.79 (dd, 2H, *J* = 8.0 Hz, *J* = 2.5 Hz, Ar-C*H*), 4.54 (d, 1H, *J* = 6.4 Hz, CH-CH_2-O*H*), 4.26–4.19 (m, 1H, $(CH_3)_2$-C*H*), 3.95 (s, 4H, Ar-CH_2), 3.61 (t, 1H, *J* = 7.6 Hz, *N*-C*H*-CH), 2.88–2.82 (q, 2H, CH_2-OH), 1.29 and 1.13 (s, 18H, Ar-C-(CH_3)$_3$) and 0.99 (d, 6H, *J* = 6.4 Hz, CH–(CH_3)$_2$). ^{13}C NMR (100 MHz; $CDCl_3$): *δ* (ppm) = 153.79, 142.87, 126.14, 125.32, 121.46, and 115.04 (Ar-*C*H), 84.47 (*N*-*C*H), 70.77 (*C*H_2-OH), 59.55 (Ar-*C*H_2), 34.05 (*C*-(CH$_3$)$_3$), 31.69 (C-(*C*H$_3$)$_3$), 28.60 (*C*H–(CH$_3$)$_2$), 20.06 and 18.83 (CH–(*C*H$_3$)$_2$). UV–Vis (λ_{max}/(nm), * = shoulder peak): 277 and 340* (C_2H_5OH); 272 and 343* ($CHCl_3$).

2.3. Synthesis of chiral boron complex (LB)

Chiral amine bis(phenolate) ligand **(L)** (3.85 g, 9.0 mmol) and 4-formyl phenyl boronic acid (1.35 g, 9.0 mmol) were mixed at 1:1 M ratio in toluene (50 mL) in a 100 mL round-bottom flask with argon (Ar) connection and refluxed with continuous stirring for 24 h using a Dean-Stark apparatus to remove the water from-product. The completion of the reaction was monitored by TLC (thin-layer chromatography) using CH_2Cl_2/CH_3OH (1:2) as a mobile phase until observing a single well-defined peak. Excess solvent was removed under the rotary evaporator and the resulting product was cooled down slowly to room temperature. Then, the retained product was washed with *n*-hexane and crystallized in $CHCl_3/C_2H_5OH$ (1:4) by slow evaporation. The precipitate was filtered under vacuum to yield the corresponding pure chiral boron complex **(LB)**.

Chiral boron complex (LB): Yield (%): 84, M.p. = 186 °C,

Elemental Analysis (calculated for $C_{34}H_{44}BNO_4$) (F.W: 541.5 g/mol) (%): C, 75.41; H, 8.19; N, 2.59. Found: C, 75.37; H, 8.16; N, 2.63. LC-MS/MS (Scan ES$^+$): *m/z* = 541.5 [M]$^+$. FT-IR (ATR, υ_{max}-cm^{-1}): 3074 υ(Ar-CH), 2961–2826 υ(Aliph-CH), 2724 υ(HC = O), 1698 υ(C═O), 1616–1557 υ(*o*-phenolate-C═C), 1502–1462 υ(Ar-C═C), 1285 υ(B-O), 1130 υ(C−O) and 954 υ(B-N). ^{1}H NMR (400 MHz; $CDCl_3$): *δ* (ppm) = 9.75 (s, 1H, Ar-C*H*O), 7.72 (d, 2H, *J* = 7.6 Hz, Ar-C*H*), 7.61 (d, 2H, *J* = 7.6 Hz, Ar-CH), 7.28 (d, 2H, *J* = 8.4 Hz, Ar-C*H*), 7.00 (s, 2H, Ar-C*H*), 6.91 (d, 2H, *J* = 8.4 Hz, Ar-C*H*), 4.30 (d, 1H, *J* = 6.4 Hz, CH-CH_2-O*H*), 3.96–3.91 (m, 1H, $(CH_3)_2$-C*H*), 3.85 (s, 4H, Ar-CH_2), 3.62 (t, 1H, *J* = 7.6 Hz, *N*-C*H*-CH), 2.98–2.83 (q, 2H, CH_2-OH), 1.28 and 1.17 (s, 18H, Ar-C-(CH_3)$_3$), 1.02 and 0.94 (d, 6H, *J* = 6.4 Hz, CH–(CH_3)$_2$). ^{13}C NMR (100 MHz; $CDCl_3$): *δ* (ppm) = 193.24 (Ar-*C*HO), 154.55, 142.30, 135.55, 132.66, 129.01, 127.40, 126.13, 124.68, 118.36, 116.94 and 114.80 (Ar-*C*H), 65.08 and 64.30 (*N*-*C*H), 58.24 (*C*H_2-OH), 48.18 (Ar-*C*H_2), 34.04 (*C*-(CH$_3$)$_3$), 31.57 (C-(*C*H$_3$)$_3$), 29.54 (*C*H–(CH$_3$)$_2$), 19.51 and 17.60 (CH–(*C*H$_3$)$_2$). UV–Vis (λ$_{max}$/(nm), * = shoulder peak): 258, 283 and 352* (C_2H_5OH); 257, 284, and 354* ($CHCl_3$).

2.4. Synthesis of salen group containing chiral boron complexes ($LB_{(1-5)}$)

Five separate 100 mL round-bottom flasks containing the solution of chiral boron complex **(LB)** (0.3 g, 0.55 mmol) in absolute ethanol solution (40 mL) were prepared. Then, 1-(3-Aminopropyl) imidazole (0.07 g, 0.55 mmol) for **(LB_1)**, *N,N*-Diethyl-*p*-phenylenediamine (0.09 g, 0.55 mmol) for **(LB_2)**, 2-Picolylamine (0.06 g, 0.55 mmol) for **(LB_3)**, 4′-Aminoacetophenone (0.08 g, 0.55 mmol) for **(LB_4)**, and 4-Amino-2,2,6,6-tetramethyl piperidine (0.06 g, 0.55 mmol) for **(LB_5)** were added in to the each separate solution. Three drops of HCOOH was added into the reaction mixture as a catalyst. The reaction mixture was refluxed for 8 h with continuous stirring and then the mixture was cooled down slowly to room temperature. The progress of the reaction was monitored by TLC as described above. Excess solvent was removed under the rotary evaporator. The obtained products were crystallized in $CHCl_3$/C_2H_5OH (1:3) by slow evaporation. Then, yellow or pale-yellow solid products, which typical colors of salen compounds, were obtained and dried in vacuo.

Complex (LB_1): Yield (%): 80, M.p. = 108 °C, Elemental Analysis (calculated for $C_{40}H_{53}BN_4O_3$) (F.W: 648.7 g/mol) (%): C, 74.06; H, 8.24; N, 8.64. Found: C, 74.01; H, 8.19; N, 8.69. LC-MS/MS (Scan ES$^+$): *m/z* = 648.7 [M]$^+$. FT-IR (ATR, υ_{max}-cm^{-1}): 3115 υ(–OH), 3046 υ(Ar-CH), 2959–2869 υ(Aliph-CH), 1643 and 1614 υ(C═N), 1598–1554 υ(*o*-phenolate-C═C), 1503–1463 υ(Ar-C═C), 1285 υ(B-O), 1131 υ(C−O) and 952 υ(B-N). ^{1}H NMR (400 MHz; $CDCl_3$): *δ* (ppm) = 9.97 (s, 1H, *H*C═N), 7.83 (s, 1H, imidazole *H*C═N), 7.79–6.98 (m, 12H, Ar-C*H* and imidazole-C*H*), 4.37 (s, 1H, CH-CH_2-O*H*), 4.09–4.01 (m, 4H, imidazole N-CH_2 and CH═N-CH_2), 3.90 (s, 4H, Ar-CH_2), 3.87–3.81 (m, 1H, $(CH_3)_2$-C*H*), 3.54 (t, 1H, *J* = 6.4 Hz, *N*-C*H*-CH), 3.07–2.98 (q, 2H, CH_2-OH), 2.05–1.96 (m, 2H, CH_2-CH_2-CH_2), 1.28 (s, 18H, Ar-C-(CH_3)$_3$), 1.07 and 0.98 (d, 6H, *J* = 6.4 Hz, CH–(CH_3)$_2$). ^{13}C NMR (100 MHz; $CDCl_3$): *δ* (ppm) = 162.72 (H*C*═N), 154.69, 142.07, 136.82, 135.95, 132.60, 129.25, 128.22, 126.30, 124.77, 119.06, 118.53, 118.11, 116.52 and 114.80 (Ar-*C*H), 64.98 and 64.40 (*N*-*C*H), 57.67 (*C*H_2-OH), 48.29 (HC═N-*C*H_2), 45.11 (Ar-*C*H_2), 43.14 (imidazole N-*C*H_2), 34.06 (*C*-(CH$_3$)$_3$), 31.62 (C-(*C*H$_3$)$_3$), 30.01 (CH_2-*C*H_2-CH_2), 29.52 (*C*H–(CH$_3$)$_2$), 19.34 and 17.60 (CH–(*C*H$_3$)$_2$). UV–Vis (λ$_{max}$/(nm), * = shoulder peak): 221, 254 and 285* (C_2H_5OH); 256, 283 and 354* ($CHCl_3$).

Complex (LB_2): Yield (%): 83, M.p. = 104 °C, Elemental Analysis (calculated for $C_{44}H_{58}BN_3O_3$) (F.W: 687.8 g/mol) (%): C, 76.84; H, 8.50; N, 6.11. Found: C, 76.80; H, 8.46; N, 6.16. LC-MS/MS (Scan ES$^+$): *m/z* = 687.8 [M]$^+$. FT-IR (ATR, υ_{max}-cm^{-1}): 3055 υ(Ar-CH), 2969–2869 υ(Aliph-CH), 1610 υ(C═N), 1591–1549 υ(*o*-phenolate-C═C), 1508–1448 υ(Ar-C═C), 1283 υ(B-O), 1149 υ(C−O) and 953 υ(B-N). ^{1}H NMR (400 MHz; $CDCl_3$): *δ* (ppm) = 9.95 (s, 1H, *H*C═N), 7.78–6.61 (m, 14H, Ar-C*H*), 4.00 (s, 4H, Ar-CH_2), 3.81 (d, 1H, *J* = 6.4 Hz, CH-CH_2-O*H*), 3.46–3.26 (m, 5H, $(CH_3)_2$-C*H* and N-CH_2), 3.18 (d, 1H, *J* = 6.8 Hz, *N*-C*H*-CH), 2.82 (s, 2H, CH_2-OH), 1.29 and 1.24 (s, 18H, Ar-C-(CH_3)$_3$), 1.13 (t, 6H, *J* = 6.4 Hz, N-CH_2–(CH_3)$_2$). 0.96 and 0.84 (d, 6H, *J* = 6.4 Hz, CH–(CH_3)$_2$). ^{13}C NMR (100 MHz; $CDCl_3$): *δ* (ppm) = 168.54 (H*C*═N), 156.20, 155.74, 142.04, 132.30, 129.93, 128.22, 127.78, 127.49, 126.58, 125.60, 124.55, 124.13, 123.06, 122.21, 118.63, 116.65, 116.00, 114.90, 112.26 and 111.13 (Ar-*C*H), 64.98 and 64.22 (*N*-*C*H), 62.47 (*C*H_2-OH), 45.68 (Ar-*C*H_2), 44.50 (N-*C*H_2), 34.03 (*C*-(CH$_3$)$_3$), 31.58 (C-(*C*H$_3$)$_3$), 29.41 (*C*H–(CH$_3$)$_2$), 19.28 and 17.60 (CH–(*C*H$_3$)$_2$), 12.67 and 12.42 (N-(CH_2-*C*H$_3$)$_2$). UV–Vis (λ$_{max}$/(nm), * = shoulder peak): 272, 322, 401, 467 and 592 (C_2H_5OH); 274, 329, 399, 481 and 596* ($CHCl_3$).

Complex (LB_3): Yield (%): 86, M.p. = 118 °C, Elemental Analysis (calculated for $C_{40}H_{50}BN_3O_3$) (F.W: 631.7 g/mol) (%): C, 76.06; H, 7.98; N, 6.65. Found: C, 76.01; H, 7.95; N, 6.71. LC-MS/MS (Scan ES$^+$): *m/z* = 631.8 [M]$^+$. FT-IR (ATR, υ_{max}-cm^{-1}): 3073 υ(Ar-CH), 2961–2869 υ(Aliph-CH), 1646 and 1611 υ(C═N), 1594–1562 υ(*o*-phenolate-C═C), 1504–1442 υ(Ar-C═C), 1282 υ(B-O), 1132 υ(C−O) and 951 υ(B-N). ^{1}H NMR (400 MHz; $CDCl_3$): *δ* (ppm) = 9.98 (s, 1H, *H*C═N), 8.45 (d, 1H, *J* = 6.8 Hz, Ar-C*H*) 7.79 (s, 2H, Ar-C*H*), 7.73–6.96 (m, 11*H*, Ar-C*H*), 4.94 (s, 2H, HC═N-CH_2), 4.36 (d, 1H, *J* = 4.8 Hz, CH-CH_2-O*H*), 3.98 (s, 4H, Ar-CH_2), 3.85–3.77 (m, 1H, $(CH_3)_2$-C*H*), 3.02 (t, 1H, *J* = 7.6 Hz, *N*-C*H*-CH), 2.08–2.03 (q, 2H, CH_2-OH), 1.34 (s, 18H, Ar-C-(CH_3)$_3$), 1.09 and 1.03 (d, 6H, *J* = 6.8 Hz, CH–(CH_3)$_2$). ^{13}C NMR (100 MHz; $CDCl_3$): *δ* (ppm) = 166.33 (H*C*═N), 155.01, 149.10, 136.82, 132.58, 132.30, 129.16, 127.84, 127.52, 127.30, 124.57, 121.61, 118.63, 116.76 and 110.08 (Ar-*C*H), 65.12 and 64.98 (*N*-*C*H), 64.07 (C═N-*C*H_2), 57.76 (*C*H_2-OH), 48.20 (Ar-*C*H_2), 34.02 (*C*-(CH$_3$)$_3$), 31.60 (C-(*C*H$_3$)$_3$), 29.63 (*C*H–(CH$_3$)$_2$), 22.77 and 17.63 (CH–(*C*H$_3$)$_2$). UV–Vis (λ$_{max}$/(nm), * = shoulder peak): 228, 258, 287* and 364* (C_2H_5OH); 242, 257, 285*, and 372* ($CHCl_3$).

Complex (LB_4): Yield (%): 82, M.p. = 237 °C, Elemental Analysis (calculated for $C_{42}H_{51}BN_2O_4$) (F.W: 658.7 g/mol) (%): C, 76.59; H, 7.80; N, 4.25. Found: C, 76.53; H, 7.76; N, 4.31. LC-MS/MS (Scan ES$^+$): *m/z* = 658.7 [M]$^+$. FT-IR (ATR, υ_{max}-cm^{-1}): 3351 υ(–OH), 3073 υ(Ar-CH), 2964–2869 υ(Aliph-CH), 1679 υ(C═O), 1629 υ(C═N), 1589–1552 υ(*o*-phenolate-C═C), 1507–1442 υ(Ar-C═C), 1280 υ(B-O), 1134 υ(C−O) and 953 υ(B-N). ^{1}H NMR (400 MHz; $CDCl_3$): *δ* (ppm) = 9.92 (s, 1H, *H*C═N), 8.11–6.73 (m, 14H, Ar-C*H*), 4.39 (d, 1H, *J* = 6.8 Hz, CH-CH_2-O*H*), 4.05 (s, 4H, Ar-CH_2), 3.88–3.72 (m, 1H, $(CH_3)_2$-C*H*), 3.07 (t, 1H, *J* = 6.8 Hz, *N*-C*H*-CH), 2.51 (s, 2H, OC-CH_3), 2.02–1.97 (q, 2H, CH_2-OH), 1.30 (s, 18H, Ar-C-(CH_3)$_3$), 1.05 and 0.98 (d, 6H, *J* = 6.4 Hz, CH–(CH_3)$_2$). ^{13}C NMR (100 MHz; $CDCl_3$): *δ* (ppm) = 176.33 (CH_3-*C*═O), 166.34 (CH_3-*C*═O), 155.01, 149.10, 136.82, 132.58, 132.30, 129.16, 127.84, 127.52, 127.30, 126.09, 124.57, 122.31, 121.61, 118.63, 116.76, and 110.08 (Ar-*C*H), 65.12 and 64.98 (*N*-*C*H), 57.76 (*C*H_2-OH), 48.20 (Ar-*C*H_2), 34.01 (*C*-(CH$_3$)$_3$), 31.60 (C-(*C*H$_3$)$_3$), 29.63 (*C*H–(CH$_3$)$_2$), 22.77 (OC-*C*H$_3$), 19.30 and 17.63 (CH–(*C*H$_3$)$_2$). UV–Vis (λ$_{max}$/(nm), * = shoulder peak): 225, 287* and 323 (C_2H_5OH); 238, 291, and 332* ($CHCl_3$).

Complex (LB_5): Yield (%): 80, M.p. = 98 °C, Elemental Analysis (calculated for $C_{43}H_{62}BN_3O_3$) (F.W: 679.8 g/mol) (%): C, 75.97; H, 9.19; N, 6.18. Found: C, 75.93; H, 9.16; N, 6.23. LC-MS/MS (Scan ES$^+$): *m/z* = 679.8 [M]$^+$. FT-IR (ATR, υ_{max}-cm^{-1}): 3221 υ(–OH), 3047 υ(Ar-CH), 2960–2795 υ(Aliph-CH), 1640 υ(C═N), 1584–1524 υ(*o*-phenolate-C═C), 1510–1465 υ(Ar-C═C), 1281 υ(B-O), 1134 υ(C−O) and 951 υ(B-N). ^{1}H NMR (400 MHz; $CDCl_3$): *δ* (ppm) = 9.95 (s, 1H, *H*C═N), 8.38 (s, 1H, Ar-C*H*), 7.80 (d, 2H, *J* = 6.8 Hz, Ar-C*H*), 7.31 (d, 2H, *J* = 6.8 Hz, Ar-CH), 6.99 (d, 2H, *J* = 6.8 Hz, Ar-C*H*), 6.75 (d, 2H, *J* = 6.8 Hz, Ar-C*H*), 4.35 (d, 1H, *J* = 6.8 Hz, CH-CH_2-O*H*), 4.06 (t, 1H, *J* = 6.8 Hz, *N*-C*H*-CH), 3.92 (s, 4H, Ar-CH_2), 3.86–3.76 (m, 1H, $(CH_3)_2$-C*H*), 3.07 (t, 1H, *J* = 6.8 Hz, HC═*N*-C*H*-CH_2), 2.05–2.02 (q, 2H, CH_2-OH), 2.04 (s, 1H, NH), 3.07 (d, 4H, *J* = 7.6 Hz, HC═*N*-CH-CH_2), 1.29 (s, 18H, Ar-C-(CH_3)$_3$), 1.09 and 1.02 (d, 6H, *J* = 5.1 Hz, CH–(CH_3)$_2$). ^{13}C NMR (100 MHz; $CDCl_3$): *δ* (ppm) = 167.83 (H*C*═N), 154.70, 142.33, 135.93, 132.81, 132.58, 129.16, 128.46, 127.62, 126.32,

124.59, 118.62, 116.51 and 114.78 (Ar-*C*H), 64.99 and 64.40 (*N*-*C*H), 60.52 (*C*H_2-OH), 55.51 (NH-*C*H–(*C*H_3)$_2$), 48.31 (Ar-*C*H_2), 43.21 (HC=*N*-CH–(*C*H_2)$_2$), 40.90 (HC=*N*-*C*H–(*C*H_2)$_2$), 34.06 (*C*-(*C*H_3)$_3$), 31.57 (C-(*C*H_3)$_3$), 29.52 (*C*H–(*C*H_3)$_2$), 25.98 and 25.50 (NH-CH–(*C*H_3)$_2$), 19.29 and 17.56 (CH–(*C*H_3)$_2$). UV–Vis (λ_{max}/(nm), * = shoulder peak): 225, 258, 283 and 358* (C_2H_5OH); 255, 285, and 360* ($CHCl_3$).

2.5. In vitro antibacterial activity screening of chiral boron complexes

The *in vitro* antibacterial activity of compounds was tested against the following organisms: *Escherichia coli* (ATCC 25922), *Bacillus cereus* (ATCC 11778), *Staphylococcus aureus* (ATCC 25923), and *Listeria monocytogenes* (ATCC 7644). The minimum inhibitory concentration (MIC) defines the lowest concentration of an antimicrobial compound that inhibits the visible growth of a microorganism. The MIC values of the chiral boron compounds were determined using the broth microdilution method based on the Clinical Laboratory Standard Institute (CLSI) guidelines M07-A9 [44] with slight modifications. Briefly, three to four discrete bacterial colonies with similar morphology selected from a 24-hour agar plate were inoculated into 4 mL sterile Luria-Bertani (LB) broth and incubated at 35 °C for a few hours. The turbidity of bacterial suspension was adjusted to 0.5 McFarland Standard (approximately 1.0 to 2.0 × 10^8 colony forming units per mL) with sterile saline. An additional 1:150 dilutions were created in Luria-Bertani (LB) broth to achieve the turbidity that each well contains approximately 5.0 × 10^5 CFU/mL after inoculation. The compounds were dissolved in Dimethyl sulfoxide (DMSO) at a concentration of at least 15 fold higher than the highest concentration to be tested and diluted the final stock concentration with LB broth so that the final concentration of DMSO during the experiment was in a safe range for strains that we used. To create a concentration gradient of each compound, the following steps were applied: 50 µL of LB broth was added in all wells of a 96-well round-bottom microdilution plate. The highest concentration of compounds in LB broth was added (50 µL) to the wells at the first row and serial two-fold-dilutions were performed by pipetting 50 µL of solution from row one to row nine. Bacteria suspension (50 µL) prepared in 15 min were added to wells in row 1–8 and 11. Each well of columns 9, 10, and 11 were served as compound sterility control, broth sterility control, and growth control, respectively. The plate was wrapped with parafilm to prevent dehydration and incubated at 35 °C for 24 h. A redox dye, resazurin, was used to determine the MIC values since each compound has an absorbance at 600 nm and turbidity-based spectroscopic detection could not be performed. After incubation, 30 µL of 0.015% resazurin was added to all wells and the plate was incubated at 35 °C for 2–4 h to observe the color change of columns from blue to pink as a result of reduction of resazurin by viable bacterial cell. The lowest concentration of compounds with no change of resazurin color was considered as the Minimum Inhibitory Concentration (MIC). Each compound was tested in duplicates in a 96-well microdilution plate and each experiment was repeated three times using three independent cultures for tested bacteria.

3. Results and discussion

3.1. Synthesis and characterization

The synthetic routes for the preparation of all targeted compounds are shown in Scheme 1-3. First, we focused on the key process to synthesize chiral amine bis(phenolate) ligand **(L)** by the reactions of 4-*tert*-butyl phenol, (R)-(-)-2-Amino-3-methyl-1-butanol, and 36% aqueous formaldehyde in 1:2:1 M ratio in refluxing ethanol/water for 24 h (Scheme 1). After that, the reaction of chiral amine bis(phenolate) ligand **(L)** and 4-formyl phenyl boronic acid in refluxing toluene for 24 h using a Dean-Stark apparatus in order to remove the water from-product gave the chiral boron complex **(LB)** (Scheme 2). Then, salen group containing chiral boron complexes **($LB_{(1-5)}$)** have been prepared by the condensation reaction of chiral boron complex **(LB)** and various primary amines in refluxing ethanol in the presence of three drops HCOOH as catalyst under mild conditions (Scheme 3). The resulting chiral amine bis(phenolate) ligand **(L)** and corresponding chiral boron complexes **(LB** and **$LB_{(1-5)}$)** were soluble in several organic solvents and compounds were stable in the solid-state. The formation of chiral amine bis(phenolate) ligand and its chiral boron complexes were fully characterized through a combination of ^{1}H and ^{13}C NMR, FT-IR, UV–Vis, LC-MS/MS spectrometry, melting point, elemental analysis, and cyclic voltammetry technique. Postulated structures of the newly prepared chiral amine bis(phenolate) ligand and its chiral boron complexes were in full agreement with their spectroscopic and elemental analyses results. Attempts to grow suitable crystals of the chiral amine bis(phenolate) ligand and its chiral boron complexes for single crystal X-Ray structures were not successful. However, the obtained spectroscopic and analytical results of chiral amine bis(phenolate) ligand and its chiral boron complexes were consistent with the proposed structure. TLC was performed to check the reaction completion and purity of compounds and the results revealed that the compounds were sufficiently pure. For the relevant spectral data associated with the synthesized chiral amine bis(phenolate) ligand **(L)** and its chiral boron complexes **(LB** and **$LB_{(1-5)}$)**, see the Supporting Information (ESI).

3.2. Spectroscopic studies

Infrared (FT-IR) spectral data were used to characterize the proposed structures of the chiral amine bis(phenolate) ligand **(L)**, the corresponding chiral boron complex **(LB)** and salen groups containing chiral boron complexes **($LB_{(1-5)}$)**. The summary of results from FT-IR analysis of the synthesized all compounds are given in the experimental section and in Figs. S1-S7. The FT-IR spectra of chiral amine bis(phenolate) ligand **(L)** showed that the υ(Ar-OH···N) vibrations are present in the region 3580–3142 cm^{-1} along with υ(C—O) at 1128 cm^{-1}. This observation indicates the formation of chiral amine bis(phenolate) ligand **(L)** by the reaction of three starting substances. On the other hand, the disappearance of υ(Ar-OH···N) band and *ortho*-phenolate or other υ(Ar-C=C) with υ(C—O) stretching vibrations shifting to a different region in chiral boron complexes **(LB** and **$LB_{(1-5)}$)** indicates the deprotonation of two (Ar-OH) groups and the coordination of two phenolic oxygen to boron center. Additionally, the appearance of two new bands at 1285–1280 cm^{-1} and 954–951 cm^{-1}, may be assigned to υ (B-O) and υ (B-N) vibrations for chiral boron complexes **(LB** and **$LB_{(1-5)}$)**,

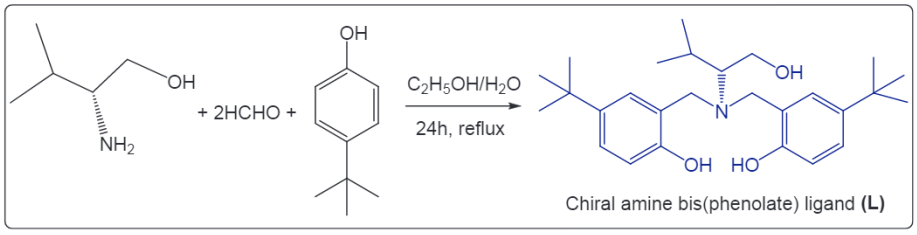

Scheme 1. Synthesis of proposed chiral amine bis (phenolate) ligand **(L)**.

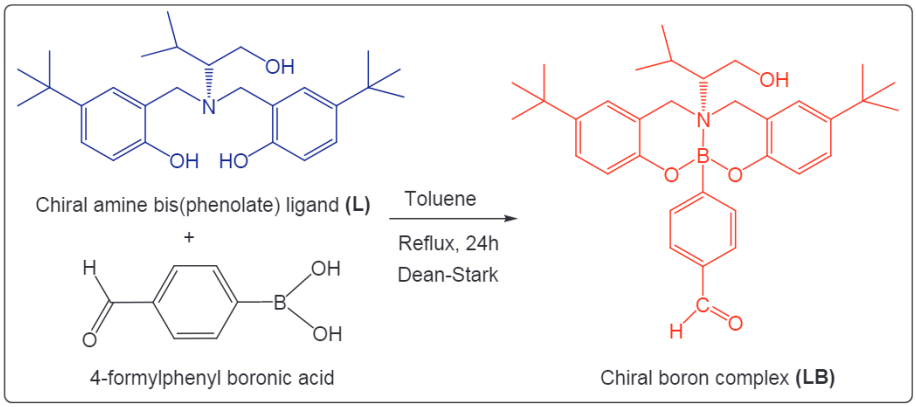

Scheme 2. Synthesis of proposed chiral boron complex **(LB)**.

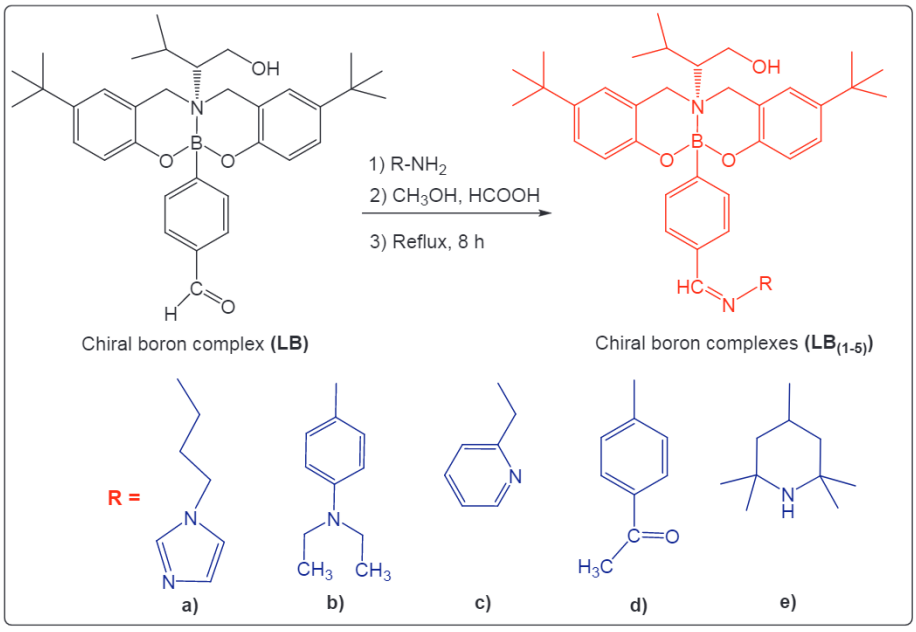

Scheme 3. Synthesis of proposed salen group containing chiral boron complexes **($LB_{(1-5)}$)** a) 1-(3-Aminopropyl)imidazole for **(LB_1)**, b) *N,N*-Diethyl-*p*-phenylenediamine for **(LB_2)**, c) 2-Picolylamine for **(LB_3)**, d) 4′-Aminoacetophenone for **(LB_4)** and e) 4-Amino-2,2,6,6-tetramethyl piperidine for **(LB_5)**, respectively.

respectively [45–47]. The other characteristic absorption band observed in the spectra of salen groups containing chiral boron complexes **($LB_{(1-5)}$)** in the region 1646–1610 cm^{-1} may be assigned to imine υ(HC═N) group [2,48], which confirms that the aldehyde group is converted to imine group in the salen group containing chiral boron complexes. Furthermore, the stretching vibrations of other groups indicate the formation of all compounds and the results are in good agreement with the proposed structures.

The UV–Vis electronic spectral measurements of the chiral amine bis(phenolate) ligand **(L)**, the corresponding chiral boron complex **(LB)** and salen group containing chiral boron complexes **($LB_{(1-5)}$)** have been recorded at the scanning range of 200 nm 1200 nm in C_2H_5OH and $CHCl_3$ solvents at room temperature. The obtained electronic transition results are presented in Figs. 1-3 and S8-S10. The maximum absorption bands of chiral amine bis(phenolate) ligand **(L)** in the range of 277–340 nm in C_2H_5OH and 272–343 nm in $CHCl_3$. Whereas, the corresponding chiral boron complex **(LB** and **$LB_{(1-5)}$)** typically display a λ_{max} value at the range of 221–592 nm for C_2H_5OH and 238–596 nm in their UV–Vis spectra which might be ascribed to the $\pi \rightarrow \pi^*$ transitions in the conjugated ring system of chiral boron complex **(LB** and **$LB_{(1-5)}$)** with $n \rightarrow \pi^*$ transition of nonbonded electrons or π-to-vacant B p-orbital transition, respectively [45]. However, the aldehyde group of

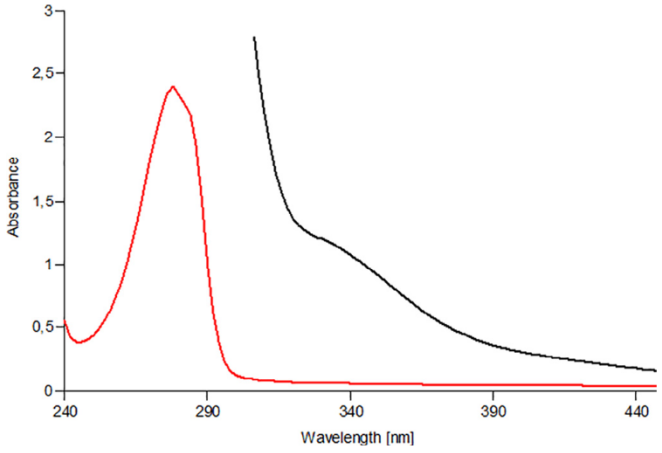

Fig. 1. UV–Vis spectrum of chiral amine bis(phenolate) ligand **(L)** in C_2H_5OH.

chiral boron complex **(LB)** is converted to imine group in the salen group containing chiral boron complexes **($LB_{(1-5)}$)** shows the significant influence on the electronic properties of **($LB_{(1-5)}$)** complexes, which indicated an effective π-conjugation in the salen group.

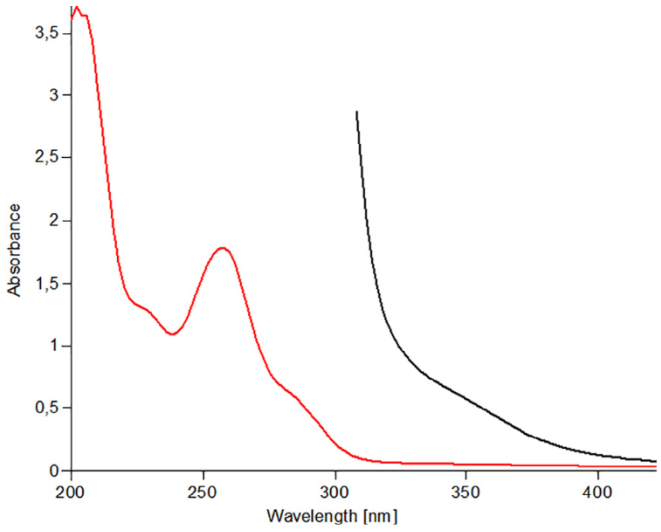

Fig. 2. UV–Vis spectrum of chiral boron complex **(LB)** in C_2H_5OH.

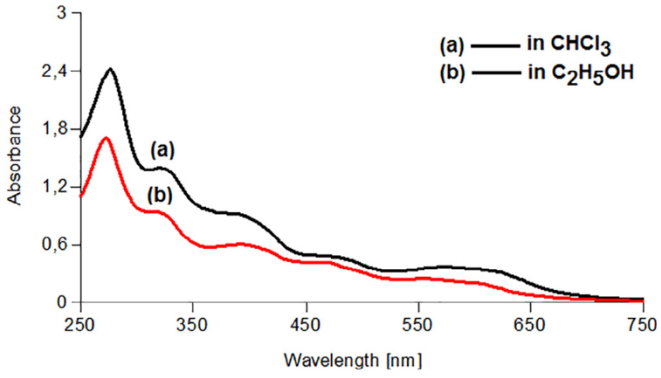

Fig. 3. UV–Vis spectrum of salen group containing chiral boron complex **(LB_2)** in C_2H_5OH and $CHCl_3$.

Additionally, compared to other chiral boron complexes, especially the electronic absorption transition of the complex **(LB_2)** has shown quite interesting results. The red-shift of the maximal absorption of **(LB_2)** compared with those of **LB**, **LB_1,** and **$LB_{(3-5)}$** complexes might be due to its relatively high polarity of the conjugated skeleton or inter-ligand charge transfer of the aromatic ring and the azomethine (–CH═N) unit.

The ^1H and ^{13}C NMR spectral results were verified that the proposed chiral amine bis(phenolate) ligand **(L)**, the corresponding chiral boron complex **(LB),** and salen group containing chiral boron complexes **($LB_{(1-5)}$)** were properly synthesized. The chemical shifts in NMR spectra of chiral amine bis(phenolate) ligand and the corresponding various chiral boron complexes in $CDCl_3$ using TMS as internal standard, unambiguously confirmed theirs proposed structures (S11-S17 and experimental part). The formation of proposed chiral amine bis (phenolate) ligand **(L)** can be easily spotted in the ^1H NMR spectrum due to the presence of D_2O exchangeable protons (Ar-O*H*) of the phenolic group around at $\delta = 8.41$ ppm as singlet and proton (CH-CH_2-O*H*) of aliphatic hydroxyl at 4.54 ppm as a doublet, respectively [49,50]. Additionally, the ^1H NMR spectra of chiral amine bis(phenolate) ligand **(L)** showed the signals of the aliphatic (CH_3)$_2$-C*H*) proton in the range 4.26–4.19 ppm, while the benzylic (CH_2) protons appeared around at $\delta = 4.90$ ppm. All other signals in the ^1H NMR spectra of chiral amine bis(phenolate) ligand **(L)** are present at their expected positions and gave suitable resonances that are in good agreement with the proposed structure. The number of carbon resonances observed in the ^{13}C NMR spectrum is in good agreement with the proposed structure of the chiral amine bis(phenolate) ligand **(L)**. On the other hand, ^{13}C NMR spectra of the newly prepared chiral amine bis(phenolate) ligand **(L)** showed new characteristic signals due to the carbons of the *N*-*C*H at $\delta = 84.47$ ppm and (Ar-CH_2) at $\delta = 59.55$ ppm. In addition, other aromatic and alkyl group carbon atoms were observed in their usual position as shown in the experimental section. Because of the ^1H NMR spectroscopic studies, the formation of chiral boron complexes was confirmed by the disappearance of the phenolic hydroxyl proton signals and chemical shifts of the aryl groups. In other words, both the phenolic O*H* group and the arylamino group are coordinated to the boron center, according to a comparison with the corresponding chemical shifts of the free chiral amine bis(phenolate) ligand **(L)**. In the ^1H NMR spectrum of chiral boron complex **(LB)**, one sharp singlet at 9.75 ppm is displayed for the Ar(*C*H*O*) unit which confirms the binding of the boron center to the two phenolic oxygen of free chiral ligand **(L)** and formation of B-O bond. However, in the ^1H NMR spectrum of salen group containing chiral boron complexes **($LB_{(1-5)}$)**, the presence of the highly deshielded resonances in the range 9.92–9.97 ppm for the characteristic azomethine (*H*C═N) proton [51], confirmed this chiral boron complexes, as expected. Moreover, the ^{13}C NMR spectra results can be analyzed in an analogous manner to that of the proton spectra and the chemical shift of ^{13}C NMR peaks supports the formation of chiral boron complex **(LB)** and salen group containing chiral boron complexes **($LB_{(1-5)}$)**. A comparison of the ^{13}C NMR results of chiral boron complex **(LB)** and salen group containing chiral boron complexes **($LB_{(1-5)}$)**, it was seen that different resonance signals in chemical shifts, which confirms the primary amines attached to the chiral boron complex **(LB)** and formation chiral boron complexes **($LB_{(1-5)}$)**. From ^{13}C NMR spectral scans, the signal for the aldehyde group carbon (Ar-*C*HO) was observed at 193.24 ppm for chiral boron complex **(LB)**, corresponding salen group containing chiral boron complexes **($LB_{(1-5)}$)** the aldehyde group is converted to the azomethine group and the characteristic azomethine group carbon resonances appeared in the range 176.33–162.72 ppm, which another evidence that the formation of the chiral boron complexes. In addition, all aromatic and alkyl group carbon atoms were observed in their usual position as shown in the experimental section.

For compounds characterization, the LC-MS/MS spectral results were confirmed the proposed structures for the chiral boron complex **(LB)** and salen group containing chiral boron complexes **($LB_{(1-5)}$)** recorded in methanol. Since the chiral amine bis(phenolate) ligand **(L)** is an oily product, the LC-MS/MS of the chiral ligand could not be taken. The LC-MS/MS of the chiral boron complexes **(LB)** and corresponding salen group containing chiral boron complexes **($LB_{(1-5)}$)** showed molecular ion peaks and characteristic fragment ions, which these results show the mononuclear nature of these chiral boron complexes. In addition, mass spectral data confirmed the appropriate isotope distribution and the isotopic distribution of parent ions in the spectra demonstrated the presence of one atom of boron in all chiral boron complexes. The fragmentation pattern is summarized in Figs. S18-S23 and in the experimental part. In light of this LC-MS/MS spectral results, the chiral boron complex **(LB)** exhibits the ion peak that is found at $m/z = 541.5$ Da $[M]^+$. On the other hand, the LC-MS/MS ion peaks of salen group containing chiral boron complexes **($LB_{(1-5)}$)** are located at $m/z = 648.7$ Da $[M]^+$ for **(LB_1)**, at $m/z = 685.4$ Da $[M]^+$ for **(LB_2)**, at $m/z = 631.8$ Da $[M]^+$ for **(LB_3)**, at $m/z = 658.7$ Da $[M]^+$ for **(LB_4)**, and at $m/z = 682.8$ Da $[M]^+$ and for **(LB_5)**, respectively.

3.3. Electrochemical studies

The electrochemical properties of chiral boron complex **(LB)** and salen group containing chiral boron complexes **($LB_{(1-5)}$)** were examined by CV. To calculate the energies of HOMO and LUMO levels of **(LB)** and **($LB_{(1-5)}$)** boron complexes, the redox potential of ferrocene (Fc/Fc^+) used as a known reference was assumed to be -4.8 eV [52]. Onset oxidation potentials (E_{ox}^{onset}) and onset reduction potentials (E_{red}^{onset}) were used to estimate the energies of HOMO and LUMO levels of each complex. The band gap HOMO ($E_g = 1234$ eVnm/λ_{max}(nm))

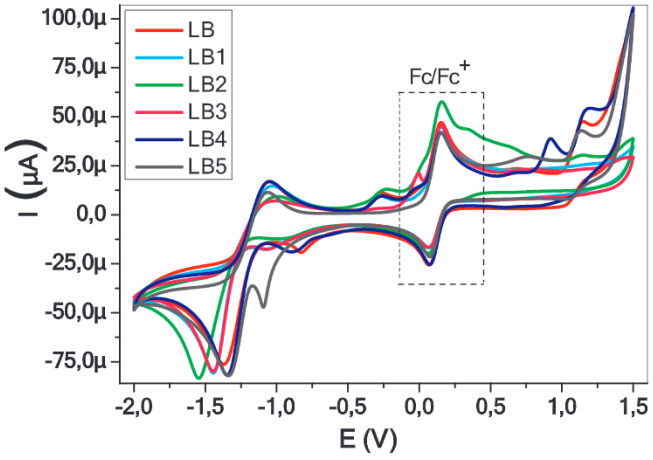

Fig. 4. Cyclic voltammograms of **(LB)** and **($LB_{(1-5)}$)** in acetonitrile solution containing 0.1 M TBATFB in the presence of 0.01 M ferrocene/ferrocenium (Fc/Fc^+) as internal standard at GC electrode. (Scan rate = 50 mVs^{-1}).

Table 1
Electrochemical data of the boron complexes **(LB** and **$LB_{(1-5)}$)**.

Complexes	E_{red} onset (V)	E_{ox} onset (v)	λ_{max} (nm)	E_g (eV)	HOMO(eV)	LUMO(eV)
(LB)	−1.28	0.58	258	4.78	−5.38	−0,60
(LB_1)	−1.31	0.56	254	4.86	−5.36	−0,50
(LB_2)	−1.37	0.53	272	4.54	−5.33	−0,79
(LB_3)	−1.36	0.54	258	4.78	−5.34	−0.56
(LB_4)	−1.33	0.53	258	4.78	−5.33	−0.55
(LB_5)	−1.35	0.52	258	4.78	−5.32	−0.54

was measured by using maximum wavelengths obtained from the UV–Vis electronic spectral measurements of **(LB)** and **($LB_{(1-5)}$)** boron complexes in the ethanol solvent, separately. The cyclic voltammograms of **(LB)** and **($LB_{(1-5)}$)** boron complexes are presented in Fig. 4 and the electrochemical data of these boron complexes are summarized in Table 1. As presented in Fig. 4, the cyclic voltammograms of **(LB)** and **($LB_{(1-5)}$)** boron complexes showed a quasi-reversible profile. The **(LB), (LB_1), (LB_2)**, and **(LB_4)** chiral boron complexes showed two reduction events, while **(LB_3)** and **(LB_5)** chiral boron complexes showed one reduction event (in the region outside the potential range of −0.12 V / 0.45 V of Fc/Fc^+ redox probe). Onset reduction potentials of **($LB_{(1-5)}$)** chiral boron complexes (E_{red}^{onset} = −1.31 V, −1.37 V, −1.36 V, −1.33 V, −1.35 V, respectively) were more negative compared to that of **(LB)** complex (E_{red}^{onset} = −1.28 V). However, the maximum wavelengths obtained from UV–Vis electronic spectral measurements were almost the same for **(LB)**, **(LB_1)** and **($LB_{(3-5)}$)** while it was interestingly different for the **(LB_2)** boron complex. Therefore, the band gap of chiral **(LB_2)** boron complex was measured at a lower value (4.54 eV) than that of **(LB)**, **(LB_1)** and **($LB_{(3-5)}$)** chiral boron complexes. Hence, experimental results obtained from the electrochemical and optical data showed that **(LB_2)** boron complex had a much lower LUMO energy level (−0.79 eV) than that of **(LB)**, **(LB_1)** and **($LB_{(3-5)}$)** chiral boron complexes. The boron complex with the lowest electrochemical LUMO level is to have the lowest band gap in UV–Vis absorbance spectroscopy [53]. In this regard, electrochemical analyzes comply with UV–Vis electronic spectral measurements. Besides, as seen in Fig. 4, it can be said that **(LB_2)** chiral boron complex catalyzes Fc/Fc^+ redox probe more due to the aromatic ring and azomethine unit involved in its structure. **(LB)**, **(LB_1)** and **(LB_5)** chiral boron complexes showed two oxidation events, **(LB_1)** and **(LB_3)** one oxidation event, **(LB_4)** three oxidation events (the region outside the potential range of −0.12 V/0.45 V of Fc/Fc^+ redox probe). Onset oxidation potentials (E_{ox}^{onset}) of the **($LB_{(3-5)}$)** chiral boron complexes are + 0.56 V, +0.53 V, +0.54 V, +0.53 V, +0.52 V, respectively, which shows that they are closer to being negative compared to the oxidation potential (E_{ox}^{onset} = +0.58 V) of **(LB)** chiral boron complex (Table 1). Thus, HOMO levels of the **($LB_{(3-5)}$)** chiral boron complexes are higher than **(LB)** chiral boron complex with minor differences (maximum 0.06 eV). In addition, *N, N*-Diethyl-*p* phenylenediamine has no significant shifting effect on the electrochemical oxidation potential [54]. Taking a stand from this result, it can be said that 2-Picolylamine, Aminoacetophenone, 4-Amino-2,2,6,6-tetramethyl piperidine structures used while deriving **(LB)** chiral boron complex do not show a significant shifting effect on their oxidation potential.

3.4. Antimicrobial activity

In vitro antibacterial activity of the chiral boron complexes **(LB** and **$LB_{(1-5)}$)** was determined against one Gram-negative and three Gram-positive bacteria strain by resazurin-aided broth microdilution method. The antibacterial effectiveness of a compound is measured by the minimum inhibitory concentration (MIC). The lowest concentration of the tested compound that inhibits the growth of bacterial strain was taken as MIC (Fig. 5). The lower MIC value means more effective antibacterial activity represented by the test compound. Table 2 presents the MIC value of each chiral boron complex **(LB** and **$LB_{(1-5)}$)** against tested bacterial strains. Since DMSO was used as a solvent, there was a limitation of the concentration that could be tested. All chiral boron complexes were prepared in a higher concentration according to their solubility to overcome the toxic effect of DMSO. The highest concentration of the chiral boron complexes that could be applied to the microdilution plate was 1024 µg/mL. All chiral boron complexes have moderate antibacterial activity against both *Escherichia coli* (ATCC 25922) and *Staphylococcus aureus* (ATCC 25923). Chiral boron **(LB_1)**, **(LB_2)** and **(LB_5)** complexes exhibited activity against *Bacillus cereus* (ATCC 11778) while **(LB)**, **(LB_3)** and **(LB_4)** had no effect. The chiral boron complex **(LB)** has a MIC value of 512 µg/mL. The addition of salen groups to the chiral boron complex **(LB)** was improved the activity of chiral boron compounds, except **(LB_3)**. Among the tested chiral boron complexes, *N,N*-Diethyl-*p*-phenylenediamine containing chiral boron complex **(LB_2)** showed the highest antimicrobial activity against all strains. The addition of *N,N*-Diethyl-*p*-phenylenediamine group to

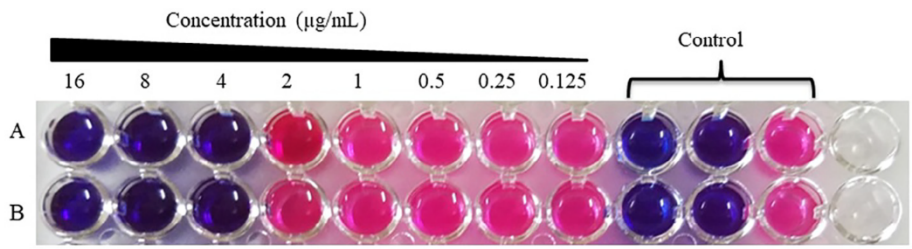

Fig. 5. An example result of the Broth microdilution method of boron complex (LB2) against *Escherichia coli. The* concentration of (LB2) decreases from 16 µg/mL to 0.125 µg/mL through column 1 to column 8. Columns 9 and 10 confirm the sterility of both media and test complexes. Column 11 is used for growth control which proves the growth of *Escherichia coli* by changing the natural blue color of resazurin to pink which is the reduced form. Row A and B are identical. The lowest concentration with no color changes in the row is taken as the MIC value (4 µg/mL). (For interpretation of the references to color in this figure legend, the reader is referred to the web version of this article.)

Table 2
Results of the MIC values for the tested boron complexes **(LB** and **$LB_{(1-5)}$)** against four bacterial strains.

	MIC Value (μg/mL)			
	G-negative		Gram-positive	
	Escherichia coli	*Bacillus cereus*	*Staphylococcus aureus*	*Listeria monocytogenes*
(LB)	512	–	512	–
(LB_1)	256	512	256	–
(LB_2)	4	4	4	512
(LB_3)	512	–	512	–
(LB_4)	512	–	256	–
(LB_5)	128	512	128	–

"-" indicates no activity against tested bacteria at the concentration of 1024 μg/mL.

the chiral boron complex dramatically increased the inhibition activity of the chiral boron complex. Moreover, the chiral **(LB_2)** boron complex was the only complex that exhibited antimicrobial activity against *Listeria monocytogenes* at the tested concentration. The obtained results of electrochemical data (Table 1) of the chiral boron complexes revealed that the chiral boron **(LB_2)** complex has the minimum calculated value of the energy gap (**E_g**) which is defined as the difference between the orbital energies of HOMO and LUMO (highest occupied molecular orbital-lowest unoccupied molecular orbital) and also the same complex is the one which represented the maximum antibacterial activity.

4. Conclusion

In this study, we describe the successful synthesis of chiral amine bis (phenolate) ligand **(L)**, its chiral boron complex **(LB)**, and salen group containing chiral boron complexes **($LB_{(1-5)}$).** Each compound was characterized by NMR (^{1}H, and ^{13}C), FT-IR, UV–Vis, LC-MS/MS spectroscopy, melting point, cyclic voltammetry as well as elemental analysis. The target chiral boron compounds **(LB** and **$LB_{(1-5)}$)** are soluble in several organic solvents and stable in the solid-state. Electrochemical studies showed that all chiral boron complexes have relatively low HOMO energies ranging from −5.32 to −5.38 eV. Also, electrochemical studies showed that 2-Picolylamine, Aminoacetophenone, 4-Amino-2,2,6,6-tetramethyl piperidine structures used while deriving chiral boron **(LB)** complex do not show a significant shifting effect on their oxidation potential. Biologically, the antibacterial potentials of the chiral boron complexes showed that *N,N*-Diethyl-*p*-phenylenediamine group containing chiral boron complex **(LB_2)** have the highest activity against all the tested bacteria strains with the lowest MIC value of 4 μg/mL and the rest showed reasonably good potential. However, this study introduced a series of chiral boron complexes antibacterial activity *in vitro*, thus are worthy of further study of developing novel drugs of promising antibacterial activity effect.

Declaration of Competing Interest

The authors declare that they have no known competing financial interests or personal relationships that could have appeared to influence the work reported in this paper.

Acknowledgment

We acknowledge gratefully the financial support from Research Fund of Harran University (HUBAP Projects No: 20006) Sanliurfa, Turkey.

Appendix A. Supplementary data

Supplementary data to this article can be found online at https://doi.org/10.1016/j.ica.2020.119777.

References

[1] A. Kilic, I.H. Kaya, I. Ozaslan, M. Aydemir, F. Durap, Catechol-type ligand containing new modular design dioxaborinane compounds: Use in the transfer hydrogenation of various ketones, Catal. Commun. 111 (2018) 42–46.
[2] A. Kilic, E. Yasar, E. Aytar, Neutral boron [(L_{1-3})BPh_2] and cationic charged boron [(L_{1a-3a})BPh_2] complexes for chemical CO_2 conversion to obtain cyclic carbonates under ambient conditions, Sustain. Energy Fuels. 3 (2019) 1066–1077.
[3] J. Lam, B.A.R. Günther, J.M. Farrell, P. Eisenberger, B.P. Bestvater, P.D. Newman, R.L. Melen, C.M. Crudden, D.W. Stephan, Chiral carbene-borane adducts: Precursors for borenium catalysts for asymmetric FLP hydrogenations, Dalt. Trans. 45 (2016) 15303–15316.
[4] J.L. Kolanowski, F. Liu, E.J. New, Fluorescent probes for the simultaneous detection of multiple analytes in biology, Chem. Soc. Rev. 47 (2018) 195–208.
[5] T.G. Drummond, M.G. Hill, J.K. Barton, Electrochemical DNA sensors, Nat. Biotechnol. 21 (2003) 1192–1199.
[6] F.L. Rock, W. Mao, A. Yaremchuk, M. Tukalo, T. Crépin, H. Zhou, Y.K. Zhang, V. Hernandez, T. Akama, S.J. Baker, J.J. Plattner, L. Shapiro, S.A. Martinis, S.J. Benkovic, S. Cusack, M.R.K. Alley, An antifungal agent inhibits an aminoacyl-tRNA synthetase by trapping tRNA in the editing site, Science 316 (80) (2007) 1759–1761.
[7] E. Sonoiki, C.L. Ng, M.C.S. Lee, D. Guo, Y.K. Zhang, Y. Zhou, M.R.K. Alley, V. Ahyong, L.M. Sanz, M.J. Lafuente-Monasterio, C. Dong, P.G. Schupp, J. Gut, J. Legac, R.A. Cooper, F.J. Gamo, J. Derisi, Y.R. Freund, D.A. Fidock, P.J. Rosenthal, A potent antimalarial benzoxaborole targets a Plasmodium falciparum cleavage and polyadenylation specificity factor homologue, Nat. Commun. 8 (2017) 14574.
[8] G.F.S. Fernandes, W.A. Denny, J.L. Dos Santos, Boron in drug design: Recent advances in the development of new therapeutic agents, Eur. J. Med. Chem. 179 (2019) 791–804.
[9] Z.A. Mangombo, P. Baker, E. Iwuoha, D. Key, Tyrosinase biosensor based on a boron-doped diamond electrode modified with a polyaniline-poly(vinyl sulfonate) composite film, Microchim. Acta. 170 (2010) 267–273.
[10] S.L. Hellstrom, J. Ugolotti, G.J.P. Britovsek, T.S. Jones, A.J.P. White, The effect of fluorination on the luminescent behaviour of 8-hydroxyquinoline boron compounds, New J. Chem. 32 (2008) 1379–1387.
[11] B.C. Das, P. Thapa, R. Karki, C. Schinke, S. Das, S. Kambhampati, S.K. Banerjee, P. Van Veldhuizen, A. Verma, L.M. Weiss, T. Evans, Boron chemicals in diagnosis and therapeutics, Future Med. Chem. 5 (2013) 653–676.
[12] H.M. Bolt, Y. Duydu, N. Başaran, K. Golka, Boron and its compounds: current biological research activities, Arch. Toxicol. 91 (2017) 2719–2722.
[13] I. Natsutani, R. Iwata, Y.S. Yamai, K. Ishida, Y. Nagaoka, T. Sumiyoshi, Design, synthesis and evaluations of spiro-fused benzoxaborin derivatives as novel boron-containing compounds, Chem. Biol. Drug Des. 93 (2019) 657–665.
[14] S.J. Baker, Y.K. Zhang, T. Akama, A. Lau, H. Zhou, V. Hernandez, W. Mao, M.R.K. Alley, V. Sanders, J.J. Plattner, Discovery of a new boron-containing antifungal agent, 5-fluoro-1,3-dihydro- 1-hydroxy-2,1-benzoxaborole (AN2690), for the potential treatment of onychomycosis, J. Med. Chem. 49 (2006) 4447–4450.
[15] H.S. Ban, H. Nakamura, Boron-based drug design, Chem. Rec. 15 (2015) 616–635.
[16] Y. Tülüce, H.D.I. Masseh, İ. Koyuncu, A. Kilic, M. Durgun, H. Özkol, Novel Fluorine Boron Hybrid Complex as Potential Antiproliferative Drugs on Colorectal Cancer Cell Line, Anticancer Agents Med. Chem. 19 (2019) 627–637.
[17] D.G. Hall, Boronic acid catalysis, Chem. Soc. Rev. 48 (2019) 3475–3496.
[18] A.I. Lozano, B. Pamplona, T. Kilich, M. Łabuda, M. Mendes, J. Pereira-Da-silva, G. García, P.M.P. Góis, F.F. da Silva, P. Limão-Vieira, The role of electron transfer in the fragmentation of phenyl and cyclohexyl boronic acids, Int. J. Mol. Sci. 20 (2019) 5578.
[19] H. İpek, J. Hacaloğlu, Synthesis and analysis of thermal characteristics of polybenzoxazine based on phenol and 3-Amino phenyl boronic acid, J. Polym. Sci. Part A Polym. Chem. 57 (2019) 1711–1716.
[20] S. Paşa, N. Arslan, N. Meriç, C. Kayan, M. Bingül, F. Durap, M. Aydemir, Boron containing chiral Schiff bases: Synthesis and catalytic activity in asymmetric transfer hydrogenation (ATH) of ketones, J. Mol. Struct. 1200 (2020) 127064.
[21] H. Abu Ali, V.M. Dembitsky, M. Srebnik, Contemporary aspects of boron: chemistry and biological applications, 1. Ed. Elsevier, 2005.
[22] J.H. Fournier, T. Maris, J.D. Wuest, W. Guo, E. Galoppini, Molecular tectonics. Use of the hydrogen bonding of boronic acids to direct supramolecular construction, J. Am. Chem. Soc. 125 (2003) 1002–1006.

[23] S. Ivankovic, R. Stojkovic, Z. Galic, B. Galic, J. Ostojic, M. Marasovic, M. Milos, In vitro and in vivo antitumor activity of the halogenated boroxine dipotassium-trioxohydroxytetrafluorotriborate ($K_2[B_3O_3F_4OH]$), J. Enzyme Inhib. Med. Chem. 30 (2015) 354–359.
[24] W. Niu, C. O'Sullivan, B.M. Rambo, M.D. Smith, J.J. Lavigne, Self-repairing polymers: Poly(dioxaborolane)s containing trigonal planar boron, Chem. Commun. 4342–4344 (2005).
[25] J. Cruz-Huerta, G. Campillo-Alvarado, H. Höpfl, P. Rodríguez-Cuamatzi, V. Reyes-Márquez, J. Guerrero-Álvarez, D. Salazar-Mendoza, N. Farfán-García, Self-Assembly of Triphenylboroxine and the Phenylboronic Ester of Pentaerythritol with Piperazine, trans-1,4-Diaminocyclohexane, and 4-Aminopyridine, Eur. J. Inorg. Chem. 2016 (2016) 355–365.
[26] P.D. Woodgate, G.M. Horner, N.P. Maynard, C.E.F. Rickard, Synthesis of dioxazaborocines from N-substituted-bis(2-hydroxyaryl)aminomethylamines, J. Organomet. Chem. 592 (2) (1999) 180–193.
[27] J. Tan, A.B. Cognetta III, D.B. Diaz, K.M. Lum, S. Adachi, S. Kundu, B.F. Cravatt, A.K. Yudin, Multicomponent mapping of boron chemotypes furnishes selective enzyme inhibitors, Nat. Commun. 8 (2017) 1760.
[28] E. Meiyanto, R.A. Susidarti, R.I. Jenie, R.Y. Utomo, D. Novitasari, F. Wulandari, M. Kirihata, Synthesis of new boron containing compound (CCB-2) based on curcumin structure and its cytotoxic effect against cancer cells, J. Appl. Pharm. Sci. 10 (2020) 60–066.
[29] M. Minozzi, G. Lattanzi, R. Benz, M.P. Costi, A. Venturelli, P. Carloni, Permeation through the cell membrane of a boron-based β-lactamase inhibitor, PLoS One. 6 (8) (2011) e23187.
[30] M.A. Soriano-Ursúa, B.C. Das, J.G. Trujillo-Ferrara, Boron-containing compounds: Chemico-biological properties and expanding medicinal potential in prevention, diagnosis and therapy, Expert Opin. Ther. Pat. 24 (2014) 485–500.
[31] M.A. Soriano-Ursúa, Chemico-Biological Activity and Medicinal Chemistry of Boron-Containing Compounds, Curr. Med. Chem. 26 (2019) 5003–5004.
[32] M. Dostani, A.H. Kianfar, M.M. Momeni, Visible light photocatalytic activity of novel Ni^{2+}, Cu^{2+} and VO_2 complexes derived from vanillin bidentate Schiff base ligand doped on TiO_2 nanoparticles, J. Mater. Sci. Mater. Electron. 28 (2017) 633–640.
[33] L. Bai, C. Gao, L. Cai, Q. Liu, Y. Qian, B. Yang, Synthesis and in vitro cytotoxicity of novel dinuclear platinum(II) complexes containing a chiral tetradentate ligand, J. Coord. Chem. 70 (2017) 3759–3768.
[34] L. Rodríguez-Silva, M. I. Fernández-García, E. Gómez-Fórneas, S. Fernández-Fariña, L. M. González-Barcia and M. J. Romero, The 21st International Electronic Conference on Synthetic Organic Chemistry session General Organic Synthesis, 1 (2017) Doi:10.3390/ecsoc-21-04774.
[35] H.C. Quilter, R.H. Drewitt, M.F. Mahon, G. Kociok-Köhn, M.D. Jones, Synthesis of Li (I), Zn(II) and Mg(II) complexes of amine bis(phenolates) and their exploitation for the ring opening polymerisation of rac-lactide, J. Organomet. Chem. 848 (2017) 325–331.
[36] E.Y. Tshuva, I. Goldberg, M. Kol, Z. Goldschmidt, Zirconium complexes of amine-bis (phenolate) ligands as catalysts for 1-hexene polymerization: Peripheral structural parameters strongly affect reactivity, Organometallics. 20 (2001) 3017–3028.
[37] S. Kannan, K.N. Kumar, R. Ramesh, Ruthenium(III) complexes of amine-bis(phenolate) ligands as catalysts for transfer hydrogenation of ketones, Polyhedron. 27 (2008) 701–708.
[38] A.J. Lough, B.J. Graziano, B.M. Wile, M. Zeller, D.J. Bettinger, Palladium(II) complexes of a bridging amine bis(phenolate) ligand featuring K^2 and K^3 coordination modes, Res. Commun. Acta Cryst. 75 (2019) 1265–1269.
[39] X.-W. Song, C. Guo, C.-N. Chen, Synthesis, Crystal Structure, and Electrochemistry of Iron and Cobalt Complexes Supported by a Pentadentate Amine-bis(phenolate) Ligand, Zeitschrift Für Anorg. Und Allg. Chemie. 643 (2017) 2110–2115.
[40] S.A. Khan, S.A.A. Nami, S.A. Bhat, A. Kareem, N. Nishat, Synthesis, characterization and antimicrobial study of polymeric transition metal complexes of Mn(II), Co(II), Ni(II), Cu(II) and Zn(II), Microb. Pathog. 110 (2017) 414–425.
[41] L. Song, X. Zhang, C. Chen, X. Liu, N. Zhang, UTSA-16 as an efficient microporous catalyst for CO_2 conversion to cyclic carbonates, Microporous Mesoporous Mater. 241 (2017) 36–42.
[42] J. Bhomia, J. Sharma, R.A. Sharma, Y. Singh, Some boron compounds of semi-carbazones: antimicrobial activity and precursor for the sol-gel transformation to nanosized boron oxide, New J. Chem. 42 (2018) 10376–10385.
[43] V. Jangir, J. Sharma, R.A. Sharma, Y.P. Singh, Some heteroleptic boron derivatives and their isomers derived from Schiff bases and glycol: synthesis, characterization and antimicrobial activities, Main Group Met. Chem. 39 (2016) 9–18.
[44] P. Wayne, CLSI. Methods for Dilution Antimicrobial Susceptibility Tests for Bacteria That Grow Aerobically;Approved Standard-Ninth Edition. CLSI document M07-A9, Clin. Lab. Stand. Inst. (2012).
[45] A. Nocentini, C.T. Supuran, J.Y. Winum, Benzoxaborole compounds for therapeutic uses: a patent review (2010–2018), Expert Opin. Ther. Pat. 28 (2018) 493–504.
[46] Y.P. Singh, P. Rupani, A. Singh, A.K. Rai, R.C. Mehrotra, R.D. Rogers, J.L. Atwood, Synthesis and IR, UV, NMR (^1H and ^{11}B), and Mass Spectral Studies of New β-Ketoamine Complexes of Boron: crystal and Molecular Structure of $OC_6H_4OBOC(R)CHC(R')NR''$ (R = p-ClC_6H_4, R' = C_6H_5, R'' = CH_3), Inorg. Chem. 25 (1986) 3076–3081.
[47] V. Jangir, R. Saharan, R. Sharma, J. Sharma, Y. Singh, Some Novel Dinuclear phenylboronates of biologically potent β-enaminoesters: Synthesis, Spectroscopic characterization, antimicrobial activity and their antiandrogenic effect, Appl. Organomet. Chem. 33 (2019) e5068.
[48] L.S. Lussier, C. Sandorfy, H. Le-Thanh, D. Vocelle, Effect of acids on the infrared spectra of the Schiff base of trans-retinal, J. Phys. Chem. 91 (1987) 2282–2287.
[49] C. Yao, Y. Yang, S. Xu, H. Ma, Potassium complexes supported by monoanionic tetradentate amino-phenolate ligands: Synthesis, structure and catalysis in the ring-opening polymerization of: Rac -lactide, Dalt. Trans. 46 (2017) 6087–6097.
[50] B.J. Graziano, E.M. Collins, N.C. McCutcheon, C.L. Griffith, N.M. Braunscheidel, T.M. Perrine, B.M. Wile, Palladium complexes bearing κ2-N, N and κ3-N, N, O pendant amine bis(phenolate) ligands, Inorg. Chim. Acta. 484 (2019) 185–196.
[51] M.S.S. Adam, O.M. El-Hady, F. Ullah, Biological and catalytic potential of sustainable low and high valent metal-Schiff base sulfonate salicylidene pincer complexes, RSC Adv. 9 (2019) 34311–34329.
[52] A. Aguiar, J. Farinhas, W. da Silva, M.E. Ghica, C.M.A. Brett, J. Morgado, A.J.F.N. Sobral, Synthesis, characterization and application of meso-substituted fluorinated boron dipyrromethenes (BODIPYs)with different styryl groups in organic photovoltaic cells, Dye. Pigment. 168 (2019) 103–110.
[53] D.L. Crossley, R. Goh, J. Cid, I. Vitorica-Yrezabal, M.L. Turner, M.J. Ingleson, Borylated Arylamine-Benzothiadiazole Donor-Acceptor Materials as Low-LUMO, Low-Band-Gap Chromophores, Organometallics 36 (2017) 2597–2604.
[54] O.V. Klymenko, D. Giovanelli, N.S. Lawrence, N.V. Rees, L. Jiang, T.G.J. Jones, R.G. Compton, The Electrochemical Oxidation of N, N-Diethyl-p-Phenylenediamine in DMF and Analytical Applications. Part I: Mechanistic Study, Electroanalysis 15 (2003) 949–960.